PRECISION RADIAL VELOCITY SPECTROMETER

Document Title	**PRVS Instrument Design and Analysis**
Document Number	PRVS-PLA-00006-0001
Issue	1.0
Date	14 September 2006

Document Prepared By:	John Rayner	**Signature and Date**	14 September 2006
Document Approved By:	David Lunney	**Signature and Date**	14 September 2006
Document Released By:	David Lunney	**Signature and Date**	14 September 2006

CHANGE RECORD

Issue	Date	Section affected	Change Description
0.1	24 July 2006		First draft
0.2	6 August 2006		Second draft
0.3	12 September 2006		Third draft
1.0	14 September 2006		First issue for Gemini review - dwl

Table of Contents

List of Figures

List of Tables

List of Abbreviations

A+G	Gemini acquisition and guidance system
FPRD	Functional and Performance Requirements Document
FOV	Field of view
FV	Fiber viewer
GCAL	Gemini facility calibration unit
GMOS	Gemini Multiple Object Spectrograph
HARPS	High Accuracy Radial velocity Planetary Searcher
HR	High (spectral) resolution
NIR	Near infrared
OAP	Off-axis parabola
OCDD	Operation Concepts Definition Document
OIWFS	On-instrument Wavefront Sensor
PRVS	Precision Radial Velocity Spectrometer
PSF	Point spread function - The response of the optical system to a point source in the object plane.
PWFS	Peripheral Wavefront Sensor
R	Spectrograph resolving power
RV	Radial velocity
XD	Cross-dispersed
SRF	Spectral Response Function - The convolution of the Point Spread Function with the geometric image of the slit, i.e. the response of a spectrograph to monochromatic radiation filling the input slit.

1. INTRODUCTION

This document discusses the major issues affecting the design of the Gemini Precision Radial Velocity Spectrograph (PRVS) and provides an overview of the resulting design. It also provides a guide to the Conceptual Design Documentation.

The document is essentially a guide to the Instrument and the 'design' journey followed in the process of the study. It provides a description of the issues considered in turn, and then discusses how those solutions were realised, or compromised, in the need to package them into a working instrument. It summarises the chosen overall design and points to relevant sections of the detailed design documentation as required.

2. APPLICABLE AND REFERENCE DOCUMENTS

Reference	Document Title	Document Number	Issue
AD01	Science Case	PRVS-SPEC-00004-0001	1.0
AD02	Science Requirements	PRVS-SPEC-00005-0001	1.0
AD03	Fibre Deployment and Acquisition System	PRVS-TRE-00007-0001	1.0
AD04	Fore-Optics and Fibre Assembly	PRVS-TRE-00002-0001	1.0
AD05	Spectrograph Assembly	PRVS-TRE-00003-0001	1.0
AD06	Infrastructure	PRVS-TRE-00001-0001	1.0
AD07	Calibration Assembly	PRVS-TRE-00004-0001	1.0
AD08	Instrument Control System	PRVS-TRE-00006-0001	1.0
AD09	Data Pipeline Software	PRVS-TRE-00005-0001	1.0

3. SCIENCE REQUIREMENTS SUMMARY

The science requirements are derived from the science described in the Science Case. To make the requirements most useful it is assumed that PRVS is a fibre-fed echelle spectrograph.

The primary science aim of PRVS is to conduct a survey of mid- to late-M dwarfs stars to search for terrestrial mass planets (~ 1-10 M_{earth}). To be useful we have concluded that several hundred stars need to be observed over multiple epochs and that the survey needs to be completed in about five years. This results in three fundamental science requirements:

- Radial velocity precision (SR_1)
- Sensitivity (SR_2)
- Observational efficiency in conducting the radial velocity survey (SR_3)

Further requirements are developed from these three fundamental requirements. The requirements derived from the three fundamental requirements have some dependence on the instrument design. By modelling the Doppler information in M dwarfs we have derived requirements for resolving power (SR_4), number of pixels per spectral resolution element (sampling) (SR_5), and simultaneous wavelength range (SR_6) required to obtain the necessary radial velocity precision. This also requires the instrument SRF to remain stable in shape and position within certain limits over the course of an individual observation and over longer periods (SR_7).

Sensitivity is a requirement for signal/noise (S/N) and therefore results in requirements for instrument throughput (SR_8) and fibre field-of-view (SR_9) (to minimize ‘slit losses’), and instrument background sources through their noise contribution (SR_10). A requirement related to throughput, stability, and observational efficiency, is for acquisition and guiding to put the target star in the centre of the fibre and to keep it there during an observation (SR_11 and SR_12). Good image quality of the target star on the entrance to the fibre is required to meet the required throughput (SR_13). Good image quality at the spectrograph detector is required to meet the required resolving power (SR_14). The cosmetic quality of the array needs to be such that the number of bad pixels does not significantly reduce the number or quality of detectable spectral features (SR_15).

The requirements of the other science cases are consistent with the science requirements derived from the primary science case for PRVS.

A complete description of the science requirements can be found in the Science Requirements document (AD02).

The science requirements are turned into detailed instrument requirements through the process of instrument design. This process is described in the relevant instrument design documents. The detailed instrument requirements are given in the Functional Performance Requirements Document (FPRD). An overview of the resulting design of PRVS is described in the following section.

4. PRVS DESIGN SOLUTIONS AND TRADE OFFS

4.1 INTRODUCTION

The fundamental requirement for PRVS is to detect earth-mass planets in orbit around low-mass stars using radial velocity measurements made in the NIR where low-mass stars are brighter. Currently there are no RV spectrographs working at wavelengths longer than the far optical and indeed some have questioned the feasibility of doing precision RV surveys in the NIR. The three main issues affecting feasibility are:

1. Possibly significantly less Doppler information in the NIR spectra of M dwarfs compared to the optical

2. Telluric contamination affecting line centroids and ultimately reducing attainable RV precision in the NIR

3. The potential lack of a suitable gas cell in the NIR for calibration

Using model stellar spectra and simulation we have shown that given the brightness of mid- to late-M dwarfs and their spectral richness in the NIR there is a significant advantage to observing them with a suitably optimized spectrograph at these wavelengths. By applying a suitable mask we have found that telluric contamination can be mitigated. For a full discussion of the modeling see the Science Case document (AD01).

For a RV spectrograph the advantage of using a gas cell inserted into the beam to provide a wavelength fiducial is that the RV calibration is inherently less sensitive to any instability in the spectrograph since spectral lines in the object to be measured travel identical light paths to the imposed fiducial absorption features. The alternative technique is to use simultaneously exposed arc lines side-by-side with the stellar spectrum. Spectrographs using the latter method need to be intrinsically more stable since the object and fiducial light paths are slightly different. Both these techniques are used successfully for planet searches at optical wavelengths; pioneered by Marcy and collaborators, and by Mayor and collaborators, respectively. It is arguable which of the two techniques is better. As explained, the gas cell method is less sensitive to spectrograph stability, and can be retrofitted to non-purpose-built spectrographs if stable enough. Disadvantages include loss of throughput and wavelength range due to the absorbing gas cell, and a complicated RV algorithm. In contrast spectrographs using the simultaneous arc line method must be purpose-built to be ultra stable. However, they do offer the advantages of higher throughput and wider wavelength range because there is no gas cell absorption, and a simpler RV algorithm. After study we have concluded there is no suitable absorption gas cell for the NIR and that consequently we need to use the simultaneous arc line method and design an ultra-stable spectrograph for PRVS.

In this study we have not considered the hybrid approach of combining interferometry with dispersive spectroscopy being developed by Erskine and collaborators (e.g. Erskine 2003, PASP 115, 225).

The most successful working instrument of the simultaneous arc line type is the High-Accuracy Radial velocity Planetary Searcher (HARPS) which became operational in 2003 on ESO's 3.6 m Telescope at La Silla (Mayor et al. 2003, The Messenger 114, 20; Rupprecht et al. 2004, SPIE 5492, 148). HARPS works in the optical and achieves a long-term RV precision of ~ 0.5 m/s. The design path to achieving this precision can be tracked by comparing HARPS with its precursors ELODIE and CORALIE (Baranne et al. 1996, AA Suppl. 119, 373), from which the design of HARPS evolved. Our goal is to make PRVS a NIR-sensitive version of HARPS, choosing similar design features to achieve the measured instrumental RV stability.

Table 1 shows the key design features and long-term RV stability of ELODIE, CORALIE, HARPS, and PRVS (proposed). All these instruments share the same basic design. Changes in design resulting in improved RV precision maybe inferred although it is not possible to directly link a particular design change to an improvement since many features change between instruments. In addition to these changes general improvements to the telescope seeing and radial velocity code were made. Design differences between HARPS and PRVS are mostly the result of working in the NIR on a large telescope (lower optical bench temperature, infrared arrays, image slicer).

	ELODIE	***CORALIE***	***HARPS***	***PRVS***
Telescope	1.9 m	1.2 m	3.6 m	8.0 m
Operational	1993	1998	2003	>2010
Optical design	Fiber-fed, bench-mounted cross-dispersed echelle (white pupil)			
Collimated beam	100 mm	100 mm	208 mm	140 mm
# fibres	2 : object + ref or sky	2 : object + ref or sky	2 : object + ref or sky	2 : object + ref
Fibre FOV	2 arcsec	2 arcsec	1 arcsec	1.4 arcsec
ADC (dispersion at 1.4 air-masses)	Yes (≈1 arcsec, 0.4 -0.8 μm)	Yes (≈1 arcsec, 0.4 -0.8 μm)	Yes (≈1 arcsec, 0.4 -0.8 μm)	Not needed (≈0.2 arcsec, 1.0-1.8μm)
Guiding	Object spill-over from fibre	Object spill-over from fibre	Object spill-over from fiber	Re-imaged object
Scrambling	Single fibre	Double fibre	Double fiber	Single fibre + mechanical agitator
Image slicing	No	No	No	Fibre slicer (7)
Echelle/ mode	R4/ Quasi-Littrow	R4/ Quasi-Littrow	R4/ Quasi-Littrow	R4/ Quasi-Littrow
XD	Prism + grism	Prism + grism	Grism	Grating
R	42,000	50,000	115,000	70,000

Sampling	1.9-2.4	3.3	3.5	>2.5
λ range	0.39-0.68 μm	0.38-0.69 μm	0.38-0.69 μm	0.99-1.75 μm
Orders	67	68	68	27
Arc lines	≈ 4000	≈ 4000	≈ 4000	≈ 300
Sep of object and ref spectra	7 pixels	13 pixels	17.3 pixels	6 pixels
Min/max inter-order gap	14/14 pixels	25/25 pixels	30/99 pixels	14/91 pixels
Detector (pixel)	1k1 (24μm)	2k2 (15 μm)	2 x 2k4(15μm)	2 x 2k2 (18μm)
Collimator	f≈850 diam≈100mm ≈f/15	f≈850mm diam≈100mm ≈f/15	f=1560mm diam=730mm ≈f/15	F=2000mm diam=580mm f/14
Camera	f=300mm f/3 5 lenses (75mm)	f=300mm f/3 5 lenses (75mm)	f=728mm f/3.3 6 lenses (225mm)	F=440mm f/3.05 6 lenses (260mm)
Image quality (R degrade)	< 1 pixel (< 10%)	< 1.5 pixel (<10%)	< 1.5 pixel (<7%)	< 0.5 pixel (<2%)
Environment	Temp controlled room	Temp controlled room	Temp controlled room + vacuum vessel (2.4 m^3)	Cryostat (2.8 m^3)
Optical bench temp	ambient ± ≈0.2K	ambient ± ≈0.2K	ambient ± 0.01K	190K ± < 0.05K
Long-term instrumental RV precision (RMS)	≈ 13 m/s	≈ 3-4 m/s	≈ 0.5 m/s	<3 m/s, goal of 1 m/s

Table 1 Key design features of the HARPS instrument series and PRVS

The most significant change between ELODIE and CORALIE (essentially the same instrument) was the change from a single fibre to a double fibre scrambler. The other change was better sampling due to smaller CCD pixels. These changes improved the long-term RV precision from ≈13 m/s to ≈3 m/s and are consistent with the expected spatial scrambling properties of the double fiber scrambler. The most significant changes between CORALIE and HARPS were the enclosure of the spectrograph in a vacuum tank and strong temperature control, a larger format CCD array to reduce scattered light effects by increasing the separation between orders, and a higher resolving power for better discrimination of features in the spectra of the target stars (typically G and K dwarfs). These changes improved the long-term RV precision from ≈3 m/s to ≈0.5 m/s.

In the following sections we will describe the design decisions that have resulted in the key design features of PRVS listed in Table 1. This will be followed by a detailed overview of the design. Our philosophy is to design PRVS to conduct a ground breaking radial velocity survey, with a minimum of R&D to minimize risk and cost, and to do so as quickly as possible.

4.2 FUNDAMENTAL LIMITS

The fundamental requirement for PRVS is to detect earth-mass planets in orbit around low-mass stars using radial velocity measurements of the primary. If it is assumed that the earth-mass planets orbit in the habitable zone (same solar constant), then velocity precisions (1σ) of 0.6 m/s, 1.5 m/s, and 2.3 m/s are required to detect earth-mass planets around 0.2 M_{sun} (~M4V), 0.1 M_{sun} (~M6V), and 0.08 M_{sun} (~M9V) dwarfs respectively (see Figure 1).

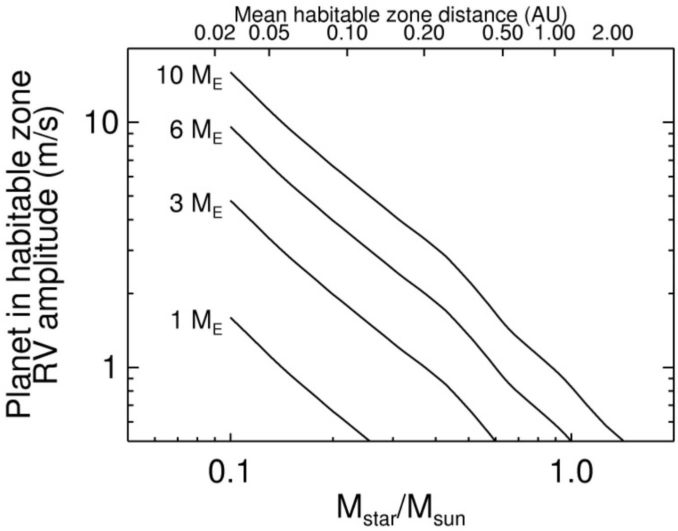

Figure 1. RV amplitude for terrestrial planets in the habitable zone, as a function of stellar mass. The mean distance of the HZ as a function of stellar mass is taken from the work of Kasting et al. (1993, Icarus 101, 108) and is indicated on the top axis. For solar-type stars, even the most massive terrestrial planets have an essentially undetected RV signature. For low-mass stars, the lighter primary stars and lower luminosities mean that habitable terrestrial planets can be detected.

Velocity precisions of ≈ 1 m/s are the current state-of-the-art in optical RV spectrographs. The flux from cool stars and brown dwarfs peaks at 1-2µm. Therefore a high-resolution near-infrared spectrograph is needed to detect earth-mass planets using the RV technique, provided that there is sufficient Doppler information in the spectra and that the stars are intrinsically stable.

The fundamental limits to detectable velocity precision are set by the Doppler information encoded in a stellar spectrum, the photon noise of the observation, and the intrinsic stability of the primary star. The amount of Doppler information depends on the depth, width and number of absorption lines recorded in the spectrum of the target star. The overall S/N depends on the total number of stellar photons recorded (flux × wavelength coverage). These factors vary with wavelength and are determined by atomic physics, temperature structure of the atmosphere, chemical abundance, and stellar rotation.

Considering photon noise only (i.e. a perfect instrument) Bouchy *et al.* (2001, AA 374, 733) show:

$$V_{RMS} \propto Q^{-1} N_e^{-0.5}, \qquad (1)$$

where the quality factor Q represents the spectral richness of the spectrum (i.e. the available Doppler information), and N_e is the total number of photo-electrons counted over the whole wavelength range (flux x bandwidth). We have used the most up-to-date models of M dwarfs to compute *Q* and RMS velocity error V_{RMS} for radial velocity measurements derived from various regions of the optical and NIR spectrum, for a range of M dwarf types and rotations (*v* sin *i*), and for a range of spectral resolving powers (R). The results are discussed in detail in the Science Case document.

In summary, we find that although *Q* values are low for the Y, J, H and K bands, the brightness of mid- and late-type M dwarfs in these bands makes the NIR superior to the optical regime for radial velocity determinations. This is particularly true if the observed star has *v* sin *i* > 5 km/s, as is typical for M dwarfs. Based on practical instrument requirements (size, cooling, array format), the simulations find the optimum combination of R, spectral sampling, and simultaneous wavelength range to be 70,000, 2.5 pixels per resolution element, and 0.99-1.75 μm, respectively.

Telluric contamination in the NIR compared to the optical is significant. In the optical telluric features deeper than about 2% are masked out to avoid variable features affecting line centroids. If the same criterion is applied to the NIR (Mauna Kea and 2mm of precipitable water) together with the requirement to mask out the barycentric velocity variation ($< \pm$ 30 km s^{-1}) centered on these features then 87% of Y, 34% of J, 58% of H, and 24% of K remains. Compared to Mauna Kea, the increased telluric absorption at Cerro Pachon due to the lower altitude results in about 10% less wavelength availability. The simulations show that for a S/N ≈ 300 velocity precisions of 1-2 m/s can be achieved by combining the Y, J and H bands. These simulations also include the effects of random velocity jitter of the telluric absorptions. Due to telluric contamination the J and K bands are less useful. Setting the long wavelength limit to 1.75 μm avoids poor telluric regions at the end of the H band window and reduces the requirements for cooling the spectrograph. The short wavelength limit of 0.99 μm is set by the telluric absorption feature at 0.92-0.98 μm. Covering wavelengths shorter than 0.9 μm would require a larger array mosaic.

Based on the Doppler information in model spectra and relative flux as a function of wavelength, the cross-over point between an optical and NIR survey (effectively PRVS:V+R versus PRVS:Y+J+H assuming the same throughput and noise) is found to be a spectral type of about M5 V. This probably an upper limit since comparisons of the models and limited high resolution data indicate more features in the observed spectra of mid- to late-M stars than in the model spectra, moving the cross-over to earlier spectral types. Our science case emphasizes surveying M5 V to M9 V stars since these lower mass stars require velocity precisions of ≈ 2 m/s to detect terrestrial mass planets in the habitable zone and therefore this survey is more robust to instrument noise. To find terrestrial mass stars in the habitable of stars earlier (more massive) than M5 V zone requires velocity precisions of ≤ ~ 1 m/s where instrument noise is a larger factor.

4.3 CALIBRATION

Optical RV spectrographs relax stability requirements by observing wavelength fiducials at the same time as the stellar measurement. There are two types of calibration scheme currently producing long-term radial velocity precisions of ~ 1 m/s.

4.3.1 Gas Cell Method

The first technique is the Gas Cell Method (Butler *et al.* 1996, PASP 108, 500) and is employed in several spectrographs notably HIRES at Keck and UCLES at the AAT. It works by superimposing the stellar spectrum with the spectrum of an iodine gas absorption cell that provides the radial velocity reference. This technique is self-calibrating since the iodine absorption spectrum provides an absolute reference and no independent spectrograph drift measurement is needed.

As discussed in the Calibration Assembly document, we have been unable to identify a suitable NIR gas cell covering the required 0.99-1.75 μm range and so PRVS will use the simultaneous arc line method.

4.3.2 Simultaneous Arc Line Method

Probably the best example of the Simultaneous Arc Line Method is the HARPS spectrograph. In this method the spectrograph is fed with two fibres. Both fibres are wavelength calibrated with Th-Ar arc lamp spectra at the beginning of the night. During an observation the first fibre carries the stellar spectrum, and on this spectrum the stellar radial velocity is computed by referring to the wavelength solution determined at the start of the night. The second fibre is illuminated with the same Th-Ar arc that was used as the wavelength fiducial. The purpose of the simultaneous arc exposure is to track any movement between the object and arc spectra since the initial calibration. The purpose of the fibres is to stabilise the photo-centres of the star and arcs on the spectrograph slit.

At the high resolving powers required for PRVS the sky background flux between the OH emission lines is less than the expected dark current and internal scatter from the sky emission lines, calibration arc lines, and object flux. Sky emission lines in the object spectra cover about 2% of the spectral coverage and therefore can be simply masked out rather than subtracted. Consequently, there is no need for a separate sky fibre. Bright moonlight is not a concern (see Figure 5).

Modelling indicates that at close to full well capacity (≈ 5×10^4 e) the measurable RMS velocity precision per arc line is about 6 m/s. In our proposed technique about 300 *simultaneously* useable arc lines in the range 0.99-1.75 μm are provided by Thorium-Argon, Krypton, Xeon, and Neon arc lamps. Using 300 arc lines results in an RMS velocity precision limit of 0.3 m/s in a 10 s exposure. These arc lines are fed into the spectrograph by a fibre. Lamp intensities are individually adjusted such that the brightest lines fill the detector well in about 0.1 s. To reach the same S/N on the faintest of these arc lines requires a minimum integration time of 10 s. Although adequate S/N is obtained on the arc lines in 10 s, the lines must be continuously read out for the duration of the science exposure so that any shift between the object spectrum and fiducial spectrum can be tracked, and also to avoid saturation. This requires a sub-array (windowed) read out of each arc line and multiple destructive reads of each sub-array during a typical science exposure (>> 10 s). The windows are read out sequentially. During the science exposure the non-windowed part of the array, on which the stellar signal falls, is continuously sampled using non-destructive reads to reduce readnoise and to determine the photon-weighted time of the exposure. Testing at UK ATC of this windowed read out mode has not shown any artefacts in the non-windowed regions of the full array (see the Detector Subsystems document). Knowing the effective time of the RV measurement to better than about 15 s is required since the earth's barycentric velocity typically changes by 1 m/s in 15 s. The only infrared array currently capable being read out in this manner is the H2RG.

Recent developments in multi-mode fiber Bragg grating technology (Bland-Hawthorn 2004, AAO Newsletter 106,4; Bland-Hawthorn 2005, AAO Newsletter 109,4) suggest they could be used to equalize the arc line intensities which would lead to a simpler array read out scheme not requiring a H2RG array. However, the technology is not considered mature enough and its use would be unacceptably risky.

In addition to tracking wavelength shifts during observing the arc lines are also used to measure the instrument SRF and to compute an accurate wavelength solution. For an RV velocity precision of 0.3 m/s RMS modelling indicates (see Science Case) the skewness (third moment of the SRF) must be known at all times to better than $\pm$0.001. The SRF must therefore be measured at many wavelengths at a S/N >1000. (The timescale for stability is discussed below.) This requires observing significantly more than the 300 arc lines that can be measured during observing. By using a range of integration times over 1000 arc lines can be measured during daytime calibration. This also meets the requirement for an accurate wavelength solution. Due to the ultra-stable nature of PRVS we expect that daytime calibration need only be done every few months or when arc lamps are changed.

Although we do not propose to use a gas cell when observing, we do plan to have one for laboratory testing purposes. The reasons are: a) to have a source with a slight resemblance to a stellar spectrum (continuum with absorption lines) for testing spectrum-fitting algorithms; b) to help measure the instrumental SRF at more positions than would be possible using the arcs alone; c) to provide a long-term velocity reference to make absolutely sure, for example, that exchanging one burnt-out arc lamp for a new one does not introduce velocity shifts at the 1 m/s level. These uses are not as demanding in the number of lines required, for example, and we expect to be able to use gas cells used in the NIR for telecommunication applications (much narrower wavelength range).

See the OCDD for details of the calibration procedures.

4.3.3 Laser Combs

The use of a laser comb generator, a repetitively-pulsed laser whose output light has a spectrum consisting of a number of narrow lines uniformly spaced in frequency, to replace arc lines, has been proposed for CODEX on ELT at optical wavelengths. This is an ideal solution for PRVS if a suitable device could be found for the NIR: it would provide a very large number of sharp lines across our entire observing spectrum, whose frequencies are accurately known and stable and whose intensities vary only moderately across the band. Such light would be perfect for the fundamental calibration of the wavelength scale of the spectrograph, for the determination of the point-spread function at every position on the detector, and for providing the reference spectrum when observing. For use in PRVS the comb frequency needs to be increased from the currently commercially available 0.1 GHz to 25-50 GHz. Our strategy is therefore to adopt the arc line system calibration and monitor developments in case a suitable generator becomes available. For a full discussion see the Science Case.

4.4 STABILITY

Although the technique of simultaneous calibration removes the need for absolute stability, experience has shown it is still critical minimise any variations in the light path. To maintain opto-mechanical stability the spectrograph is mounted on a vibration-isolated optical bench. The bench is contained inside a cryostat and cooled to 190K for low background operation. The optical bench is temperature stabilised to minimise movement due to temperature changes. Operating in a vacuum also removes variations due to air pressure (refractive index) changes in the light path of the spectrograph. Feeding the spectrograph with an optical fibre from the telescope serves two purposes. First, it allows more freedom in the size and location of the spectrograph. Second, the spatial scrambling properties of the fibre stabilise the photo-centre of the star in the slit of the spectrograph. This is critical for a spectrograph like PRVS in which the calibration path is not identical to the science path. Accurate guiding of the target star on the entrance of the fibre further stabilises the photo-centre of the star in the slit.

4.4.1 Opto-mechanical Stability

A full mathematical analysis of the requirements for stability is given in the Science Case document. To keep the RV precision to < 1 m/s due to changes in the skewness (third moment) of the SRF any drift of the image of the spectrum over the face of the detector must be < 0.1 pixel during the course of any observation (typically from a few minutes up to one hour). A further requirement is to measure the instrument SRF to $\pm$ 0.001 (S/N=1000) and for the SRF to change by not more than this between the time of the science observation and the measurement of the SRF during daytime calibration. Based on experience with HARPS we expect that daytime calibration will be required only once every few months.

Temperature drifts affect the precision in much the same way as mechanical flexure, and so they too should be kept down to < 0.1 pixel. The components most sensitive to temperature drifts are the gratings. For an echelle grating on Zerodur the temperature should be kept stable to within ± 5 K. To keep the SRF stable to ± 0.001 modelling of thermal changes in the refractive camera indicates that the temperature should be stable to ±0.05 K. Therefore the temperature stability specification is set by SRF stability and the requirement for the cold structure is < ±0.05 K.

It is also interesting to consider the gains obtained by operating the spectrograph in a vacuum. With PRVS at one atmosphere typical daily pressure variations (10 mbar or 1%) shift the spectrum by about 1000 m/s (0.25 pixels) and broaden the SRF due to focus changes. Most of this variation is removed by simultaneous calibration but residuals limit precision. Some of the improvement between CORALIE and HARPS is due to vacuum operation (see Table 1).

Analysis of the affects of vibration (see the Science Case document), coming principally from closed-cycle coolers attached to the cryostat, leads to the conclusion that SRF broadening due to vibration should be kept < 0.1 pixel.

4.4.2 Fibre Feed and Spatial Scrambling

Any movement of the photo-centre of the star in the spectrograph slit will result in radial velocity errors. At the resolving power of 70,000 the slit has a width of 4300 m/s and so to obtain a velocity precision < 1 m/s the spatial position of the photo-centre in the slit must be stabilised to better than 1/4300 of the projected slit width on the sky. This is achieved by using the spatial scrambling properties of the fibre feed and by accurate guiding.

Single fibres scramble spatial information by a factor of about 22. Double-fibre scramblers (Hunter & Ramsey 1992, PASP 104, 1244), which consist of two fibres in series plus transfer optics, scramble spatial information by about 500 ($\sim 22^2$). The order of magnitude improvement in precision of CORALIE over ELODIE (see Table 1) was primarily the result of using a double-fibre scrambler. However, the scrambling gain is improved at the expense the throughput. Recent experiments by Avila et al (Orlando SPIE, 2006) have demonstrated scrambling gains in single fibres (diameters > 200 μm) of about 1000 when the fibre is mechanically vibrated. We propose to use this technique in PVRS. The improvement in overall system throughput over a double-scrambler is about 25%.

Guiding of the target star on the input to the fibre can further stabilise the photo-centre on the slit by a factor of 10. As result we expect the combination of scrambling and guiding to reduce photo-centre errors to < 1 m/s.

Modal noise in fibres (due to movement of the fibre as the telescope tracks) is known to limit S/N < 150-400 (Baudrand & Walker 2001, PASP 113, 851, and Grupp 2003, A&A 412, 897), depending on the degree of vignetting in the spectrograph. This noise is completely eliminated by continuous, low-amplitude mechanical agitation of the fibre. In PRVS the mechanical agitator removes modal noise and increases spatial scrambling.

4.4.3 Acquisition and Guiding

In the Gemini Announcement of Opportunity for PRVS it was anticipated that light would be collected in a fibre interface mounted in the GMOS mask cartridge (like bHROS) and transferred to PRVS by optical fibre. In this scheme a spiral dithering scheme would be used to peak up the target star in the fibre, a procedure which can take 5 to 10 minutes depending on brightness. Guiding would be done by the GMOS OIWS but on another star in the field available to the OIWS.

Since swift object acquisition is essential for the overall efficiency of the radial velocity survey, and since accurate guiding is needed to meet the required radial velocity precision, we have concluded that these objectives are best met with a CCD fibre viewer (FV). Since there is not room for the FV in the GMOS/bHROS scheme, the FV and optical fibre interface are located next to GCAL, and fed by a pick-off mirror. A focal-reducing lens re-images the telescope focal plane onto the entrance to the fibre and a bare CaF_2 in the optical beam behind the lens partially reflects the beam onto a CCD. All these components are mounted rigidly in one structure and do not move. Acquisition is done with the 30″x30″ field of the CCD and the science target is placed on the CCD location mapped to the centre of the fibre. Acquisition should take less than a minute. Fast guiding (~30Hz), astigmatism and slow focus correction, is done with the PWFS. Slow guiding corrections for flexure between the PWFS and FV/object fibre are done with the CCD (< 0.3 Hz) via a socket connection to the telescope control system. Slow guiding can start while the PWFS correction loop converges (which may take a few minutes).

Locating the acquisition and guiding components of PRVS next to GCAL has the added advantage of not using an assigned ISS instrument port. This means that PRVS is always available and can respond to target of opportunity requests such as Gamma Ray Bursts events (see GRB observing scenario in OCDD).

4.5 HIGH RESOLUTION SPECTROSCOPY

The resolving power of an astronomical grating spectrograph is given by

$$R = \frac{2nd}{\varphi_s D} \tan \theta_B \,, \qquad (2)$$

where d is the diameter of the collimated beam, ϕ_S is the projected slit width or fibre diameter (in radians), D is the diameter of the telescope, θ_B is the blaze angle of the grating, and n is the refractive index of the transparent medium in which the grating is placed. For traditional astronomical spectrographs operated in air or vacuum n is 1.0.

From the modelling of stellar spectra together with practical requirements for the spectrograph (size, cooling, array format) a good compromise for the resolving power is R=70,000. In median seeing conditions (about 0.6″ at J) a fibre diameter of 1.2″ is the minimum acceptable size to ensure low light loss. For off-the-shelf gratings the largest available blaze angle is 76.0° (R4). With these parameters the collimated beam diameter on Gemini (D = 8 m) is 420 mm, requiring spectrograph collimator focal lengths of 6 m for reasonable optical performance (~f/15). The resulting instrument envelope is too large even for the Gemini pier lab even without the difficulty of cooling and stabilising such a large instrument.

From Equation (2) there are three parameters that can be changed to reduce the collimated beam diameter and corresponding instrument size. These are the grating blaze angle, the refractive index by using an immersion grating, and the projected slit width by using an image slicer. As explained below, our chosen solution is to use a standard R4 echelle grating and an image slicer.

4.5.1 Gratings

One option is to reduce the collimated beam diameter by using a very high grating blaze angle. However, this results in coarse gratings that are difficult to fabricate, and format problems arising from the large change resolving power across orders. Consequently, this approach was not considered viable.

Another option is to use an immersion grating made from GaAs (n=3.3, transmission 0.8-12µm). This reduces the beam diameter to an acceptable 130 mm. A diamond-machined GaAs immersion grating was found to be a potentially viable technology in our study for HRNIRS, but only after further research and development. One significant drawback of immersion gratings is the increase in effective speed of the collimating spectrograph optics due to expansion of the dispersed beam on emerging from the high index material. This property of high index immersion gratings drives much of the detailed optical design.

Our chosen solution is to use a standard R4 echelle grating and to reduce the slit width at the entrance to the spectrograph by using an image slicer.

4.5.2 Image Slicing

Two options were considered for image slicing, a Modified Bowen-Walraven image slicer (Simmons et al. 1982, SPIE 331, 427), and an optical fibre image slicer. The objective of both slicers is to slice the output of the fibre into three slices and recombine these into a long slit, reducing the width of the spectrograph by a factor of three, and the collimated beam diameter to an acceptable 140 mm.

The Modified Bowen-Walraven image slicer consists of a glass slicer plate and glass prism cemented together. An inclined interface between the slicer plate and the prism slices up the input and total internal reflection at the prism/slicer interface reformats the output into a long slit. The device is optically very efficient. However, in our application it suffers from two significant problems. First, only one slice is in focus, and so it works best at slow focal ratios. To reduce focal ratio degradation the fibre is fed at a fast f/5.5 and additional optics would be needed to use the Bowen-Walraven slicer. Second, the illumination of each slice is different and so the photo-centre of the slit varies along its length.

Our solution is to image the output of the 300 μm diameter fibre from the telescope onto a bundle of seven 100 μm diameter fibres. These are arranged in three columns of two, three, and two fibres, and combined into a seven-fibre-long slit at the entrance to the spectrograph. This device solves the problems encountered with the Modified Bowen-Walraven image slicer, although the efficiency is lower due to the finite packing fraction of the fibre bundle (68%).

A disadvantage of image slicing in general is that the increased slit length requires a larger format detector, or fewer orders, or less space between orders.

4.5.3 Cross Dispersion and Array Format

To fit 0.99-1.75 μm at a well-sampled resolving power of R=70,000 onto any practical NIR array or array mosaic requires cross dispersion. In general prisms are the best solution since they are purely refractive devices without any grating efficiency function and therefore cover a wide wavelength range at very high efficiency. With the right choice of prism material, spectral order spacing can be made uniform for optimum use of array format. In practice prisms can be difficult to implement due to their limited dispersion. This can require the use of several prisms in series. In contrast gratings (or grisms) are simple to implement and by selecting an appropriate line frequency any dispersion can be obtained. However, efficiency and wavelength range are limited, and the uneven spacing of spectral orders can lead to less than optimum use of array format. (ELODIE and CORALIE used a combination of prism and grating to create a constant dispersion device to keep the order spacing uniform and were therefore able to use smaller format CCDs.) We have investigated in some detail prism and grating designs.

As expected a cross-dispersing grating design was easy to implement. With an R4 echelle grating (31.6 lines/mm) and a cross-dispersing first-order reflection grating (100 lines/mm), 0.99-1.75 μm is covered in 27 orders on a 1x2 mosaic of 2048x2048 H2RG detectors (18 μm pixels) (see Figure 2). The minimum inter-order gap is 14 pixels increasing to 91 pixels at the long wavelength limit, and the gap between the reference arc spectrum and the object spectrum is 6 pixels. Larger gaps are preferred to reduce scattering into neighbouring orders, and finite gaps are required to fit and remove any scattered light. We consider these separations marginal but acceptable. An order sorting filter is needed to prevent side-lobe contamination at about 1.0 μm from the second order of the cross disperser.

Note the orders do not fit perfectly onto the mosaic. This is a compromise between using an off-the-shelf grating and an expensive custom ruling. Also, there is a 2.5mm gap (~150 pixels) between the two butted detectors. The total loss of wavelength coverage due to these effects is 20% at H, 3% at J, and 3% at Y. However, the loss of wavelength coverage does not significantly reduce the amount of Doppler information acquired.

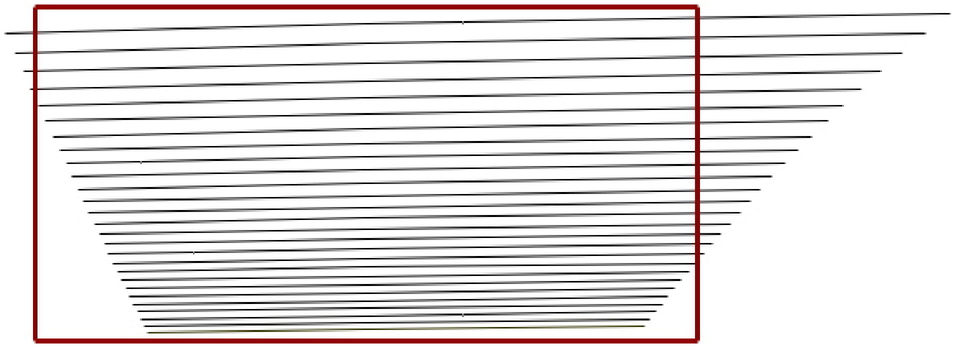

Figure 2. The 2 x 1 array XD spectral format

It is easy to increase the dispersion of the cross-dispersing grating (220 lines/mm) to increase these separations. Any increase requires a jump to a 2x2 array mosaic (see Figure 3) and slightly bigger camera lenses. This is a direct risk versus cost trade.

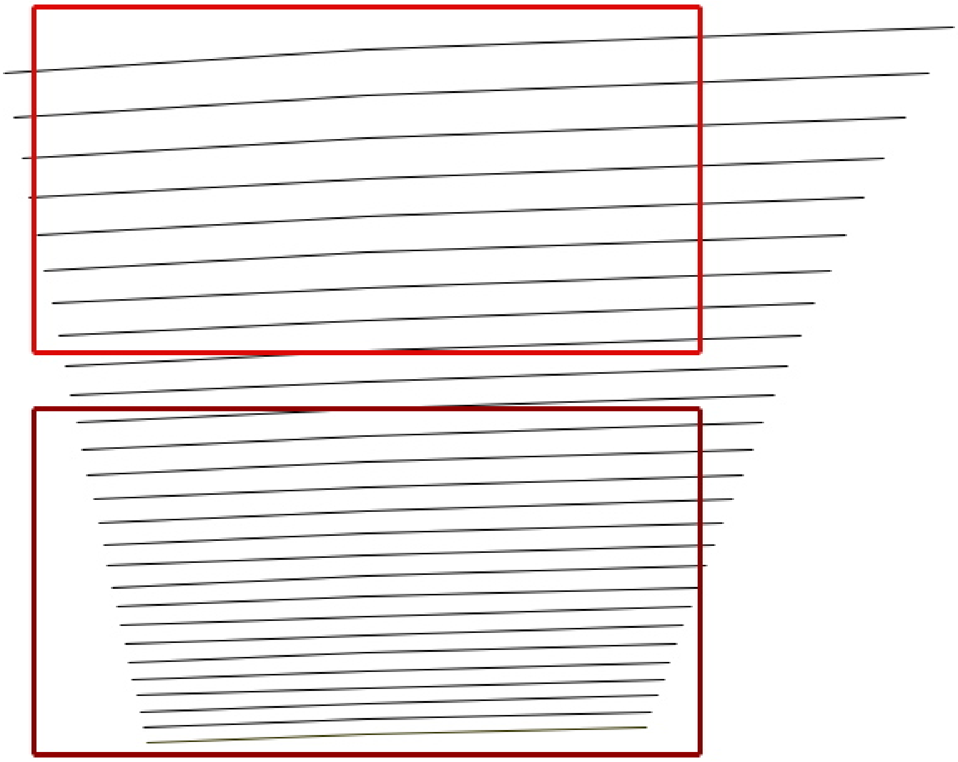

Figure 3. The 2 x 2 array XD spectral format. The 6 mm gap between the top-half and bottom-half of the mosaic allows better spacing of the orders since orders lying in the wide telluric absorption between the J and H bands can be placed in the gap.

In principle the use of prisms can increase the throughput by a factor of about two due to their greater efficiency over a wide wavelength range, and since there is no need for separate order sorting. Our best design required the use of three 45° SF57 prisms in series to get a somewhat less than optimum dispersion across a 1x2 mosaic of H2RG detectors (see Figure 4). Internal absorption due to the large path length in the SF57 prism material, the only material found with the required dispersion in the 0.98-1.75 μm range, somewhat reduced the expected throughput advantage of the prism at wavelengths longer than about 1.5μm. Also, extra optical aberrations were introduced due to the inability to place all the prisms at the white pupil. This required the addition of three extra lenses to reduce aberrations to the level of the grating design. Absorption in these extra lenses negates the throughput advantage of the prism design. At ~20 Kg each the prisms are very bulky. In contrast to the grating design it is also very difficult to increase dispersion enough to use a 2x2 array mosaic for increased order spacing.

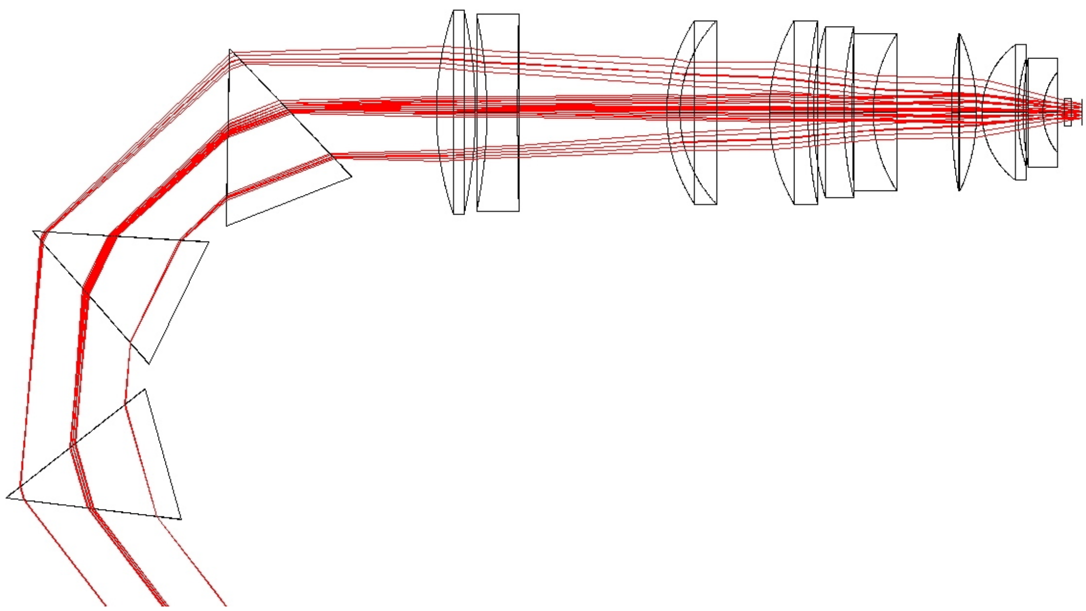

Figure 4. Prism cross dispersion design

Although the performance of the grating and prism designs turns out to be similar, the much greater simplicity and flexibility of the grating design lead us to use it in PRVS.

4.5.4 White Pupil Spectrograph

The spectrograph is of the white pupil design, like most other working radial velocity spectrographs (e.g. UVES on VLT, HIRES on Keck, UCLES on AAT, and HARPS). This design is optimum for optical stability since both the echelle grating and the cross-dispersing grating are located at pupils. It also minimises the size of both gratings and the camera. The white pupil configuration allows the echelle grating to work at close to maximum efficiency since only a small tilt of the grating is required for the exiting beam to clear the incoming beam.

4.6 SENSITIVITY MODEL

A sensitivity model of PRVS is used to understand instrument requirements such as throughput, instrument background, and detector performance, needed to accomplish the Science Case. Using the estimated sensitivity mock RV surveys have been constructed. The OCDD gives details of these surveys and how PRVS will be used to execute them.

4.6.1 Science Derived Input Parameters

Science Requirements that are needed to estimate sensitivity are given Table 2.

Parameter	
Resolving power (R)	70,000
Spectral sampling	2.5 pixels
Wavelength coverage	0.99-1.75 μm
Fibre FOV	1.41″
Pseudo-slit length	17.5 pixels

Table 2 Science Derived Sensitivity Parameters

4.6.2 System Throughput

The total system throughput is estimated from the transmission of the components in the optical design. These and the QE of the detector are tabulated in Table 3. Details of the optical designs of the various components can be found in the design documents for the Fibre Deployment and Acquisition System, the Fore-optics Fibre Assembly and the Spectrograph.

Component	Transmission	Comment
TELESCOPE AND FIBRE DEPLOYMENT SYSTEM		
Primary mirror	0.99	
Secondary mirror	0.99	
Science fold mirror	0.98	45° inclination
Pickoff mirror	0.98	45° inclination
Focal reducer doublet	0.94	0.985^4, 4 surfaces 1.5% loss per surface
CaF_2 substrate	0.97	0.985^2
	0.86	
FIBRE FEED		
Fibre 1.4″ FOV	0.98	For 0.6″ seeing at J, (median), 2% spill-over
Fibre 1.4″ FOV	(0.88)	For 0.8″ seeing at J, 12% spill-over
Coupling efficiency	0.90	Focal ratio degradation factor
Fibre 1 input	0.985	

Fibre 1 internal transmission	0.985			≈ 40 m length
Fibre 2 output	0.985			
Split fibre at cryostat				
Transfer lens 1	0.97			0.985^2
Transfer lens 2	0.97			0.985^2
Coupling efficiency	0.90			Focal ratio degradation factor
Fibre 2 input	0.985			
Fibre 2 internal transmission	1.00			≈ 1 m length
Fibre 2 output	0.985			
	0.69			
IMAGE SLICER				
Packing fraction	0.76			7 x 110/100μm fibres with 315/300μm fibre
Epoxy interface	0.985			
Internal transmission	0.995			≈ 1 m length, small cladding thickness
Fibre output	0.985			
	0.73			
SPECTROGRAPH	Y	J	H	
Focal reducer doublet	0.94	0.94	0.94	
Fold mirror	0.98	0.98	0.98	
Collimator, first pass	0.99	0.99	0.99	
Echelle grating	0.71	0.70	0.59	Quasi-Littrow mode, blaze peaks
Collimator, second pass	0.99	0.99	0.99	
Slit mirror/fold	0.99	0.99	0.99	
Collimator, third pass	0.99	0.99	0.99	
XD grating	0.69	0.84	0.77	First order grating
Camera (6 lenses)	0.83	0.83	0.83	0.985^{12}, 12 surfaces 1.5% loss per surface
Camera internal transmission	0.995	0.990	0.990	≈ 6 x 25 mm
Order sorting filter	0.80	0.80	0.80	0.99-1.75μm, to reject second order from XD
	0.29	**0.34**	**0.27**	
QE H2RG detector	**0.91**	**0.91**	**0.93**	Measurements of SNAP device
Total system throughput	**0.11**	**0.14**	**0.11**	At echelle blaze peaks

Table 3 System Throughput

The total system throughput is given at the blaze peaks at the centre of the Y, J, and H bands (see Table 3). Due to the blaze function the throughput is less at the edge of the orders. However, these wavelengths are measured twice and so the average throughput is closer to the blaze peaks. A throughput of 0.1 is used in the sensitivity model.

4.6.3 Sky Background

The atmospheric transmission code ATRAN was used to compute a telluric transmission spectrum (R=70,000) for an air mass of 1.15 (60° elevation) and 2 mm of precipitable water (average for Mauna Kea). Thermal emission from the sky was calculated by assuming a sky emissivity of (1 – sky transmission) and a sky temperature of 260 K. Estimates of the non-thermal continuum between the OH lines are from Maihara et al. (1993, PASP 105, 940). OH emission lines are not included since they illuminate only a few percent of pixels at these resolving powers and these regions are masked out in data reduction. However, since a few tens of the lines are very bright an internally scattered OH instrument background is estimated (see below). Estimates of the sky brightness due to the moon come from the Gemini website.

4.6.4 Telescope Background

Thermal background from the telescope and warm fibres are calculated assuming a temperature of 273 K and an emissivity of 0.1.

4.6.5 Detector Performance

Estimates for the quantum efficiency (QE) come from measurements of a H2RG device for the Super-Nova/Acceleration Probe (SNAP) project (Schubnell et al. 2003, SPIE 6276, 62760Q). Experience with H2RG devices at UK ATC and UH indicates that readnoise in the range 5-10 e RMS with multiple non-destructive reads (NDRs) and dark currents at the level 0.01 e/s are standard when operated at 60-70 K. Persistence is a potential issue for H2RG devices but as long as saturation is avoided persistence currents can be kept well below 1 e/s (see Detector Subsystem document). Sensitivity for a range of detector parameters is given in Table 4.

4.6.6 Instrument Background

The flux from the faintest RV targets (J~12) is about 0.5 photo-electrons/s/pixel, and the flux is even lower in some of the secondary science cases. Therefore it is important for the detector to have a low dark current and for the thermal background from the instrument to be even lower. At resolving powers of ~ R=70,000 at ~1-2μm there is effectively no background from the sky in between the sparse OH emission lines. Most of the background comes from detector dark current and any light scattered inside the instrument (see Figure 5). Consequently, there is no need for a separate sky fibre. Estimates for the scattered light background come from considering the light reflected from the detector onto the camera lenses and back onto the detector for both OH emission lines and the simultaneously exposed arc lines. It is assumed that the reflected background fills the array. These are probably upper limits since the reflected background will probably overfill the array or otherwise appear as confined ghost images. (Ghost analysis is being done as part of the optical design and will be incorporated in this analysis later.) The optical bench is cooled to about 190K to keep the instrument thermal background comfortably below the dark current. The total background in Figure 5 is the sum of all the given backgrounds. In decreasing magnitude (λ < 1.8μm) these are: scattered arc lines

(0.02 e/s), dark current (0.01 e/s), grey moon, optical bench at 190K, and non-thermal emission from the sky.

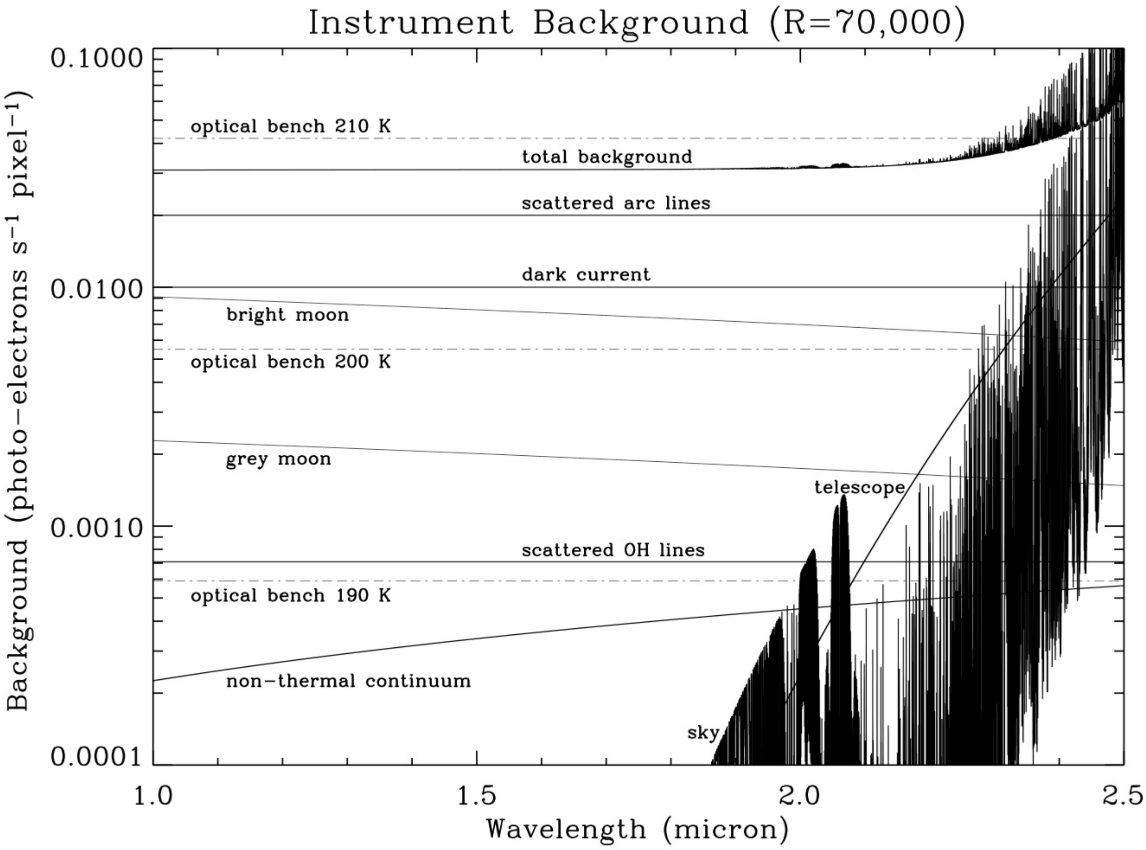

Figure 5. Instrument background

4.6.7 Estimated Sensitivity

Table 4 tabulates the effect of readnoise and dark current on sensitivity in the RV mode (300σ), assuming a system throughput (sky + telescope + instrument + detector) of 0.10 and the backgrounds discussed above. Sensitivity is measured away from OH emission lines and telluric features. The sensitivity assumes a flat-fielding accuracy of better than 0.5% per pixel. Note that sensitivity is not a strong function of detector readnoise and dark current due to the highly signal-limited (300σ) nature of the RV observations until the dark current (or total background) approaches 1.0 e/s. Conservative values for the readnoise (10 e RMS) and dark current (0.1 e/s to include persistence) are assumed for the RV observing scenarios given in the OCDD.

Readnoise (e RMS)	Dark current (e/s)	Y	J	H
10.0	1.00	11.57	11.02	10.48
10.0	0.10	12.00	11.44	10.91
10.0	0.01	12.08	11.53	10.98
5.0	1.00	11.65	11.11	10.56
5.0	0.10	12.26	11.71	11.17
5.0	0.01	12.41	11.86	11.31

Table 4 R=70,000 one-hour 300σ (600 s on chip) continuum sensitivity (Vega magnitudes)

In contrast the sensitivity is more sensitive to detector performance when observations are not so strongly signal-limited as will be the case for many of the non RV mode programs (30σ). In this case the calibration arc lines are not simultaneously exposed and this component of the instrument background is removed, improving the sensitivity. The continuum sensitivity is tabulated in Table 5 and the corresponding line sensitivity is tabulated in Table 6. Again, conservative values for the readnoise (10 e RMS) and dark current (0.1 e/s) are assumed for the GRB observing scenario given in the OCDD.

Readnoise (e RMS)	Dark current (e/s)	Y	J	H
10.0	1.00	14.28	13.73	13.19
10.0	0.10	14.87	14.32	13.78
10.0	0.01	14.99	14.44	13.90
5.0	1.00	14.39	13.84	13.30
5.0	0.10	15.30	14.76	14.22
5.0	0.01	15.65	15.11	14.56

Table 5 R=70,000 one-hour 30σ (600 s on chip) continuum sensitivity (Vega magnitudes)

Readnoise (e RMS)	Dark current (e/s)	Y	J	H
10.0	1.00	2.30×10^{-16}	1.90×10^{-16}	1.44×10^{-16}
10.0	0.10	1.34×10^{-16}	1.11×10^{-16}	8.38×10^{-17}
10.0	0.01	1.20×10^{-16}	9.90×10^{-17}	7.50×10^{-17}
5.0	1.00	2.08×10^{-16}	1.72×10^{-16}	1.30×10^{-16}
5.0	0.10	8.90×10^{-17}	7.37×10^{-17}	5.59×10^{-17}
5.0	0.01	6.48×10^{-17}	5.36×10^{-17}	4.07×10^{-17}

Table 6 R=70,000 one-hour 30σ (600 s on chip) line sensitivity (Vega magnitudes)

4.6.8 Guider Sensitivity

The function of the guider is accurately place RV target stars on the centre of the fibre and keep them there. The guider sends slow corrections (< 1 Hz) to the telescope to account for any flexure between the Fibre Deployment and Acquisition System and the PWFS. The PWFS provides fast (~30 Hz) guiding for control of tip/tilt, slow focus and astigmatism.

To guide at 1 Hz on the faintest objects in the survey requires a S/N > 20 in 1 s. A simple, cost effective way to do this is with a red sensitive CCD in the Z band where M and L dwarfs are brightest. (We avoided NIR cameras since they require more cooling and space is limited around GCAL.) The faintest stars in the nominal RV survey (see OCDD) have a Z magnitude of 14.8 (L2 at ~6 pc). The total system throughput of the guider is estimated from the transmission of the components in the optical design. These and the QE of the CCD are tabulated in Table 7.

Component	Transmission	Comment
Primary mirror	0.99	
Secondary mirror	0.99	
Science fold mirror	0.98	45° inclination
Pick-off mirror	0.98	45° inclination
Focal reducer doublet	0.94	0.985^4, 4 surfaces 1.5% loss per surface
CaF_2 substrate	0.015	Low reflection, optimised for spectrograph channel
Z-band filter	0.80	0.83-1.00μm
CCD QE	0.50	
Total guider throughput	**0.007**	At Z

Table 7 Guider Throughput

An anti-reflection coated CaF_2 substrate is used to reflect light to the CCD guider in order to maximise throughput of the spectrograph. With a throughput of 0.007 and an off-the-shelf CCD system (dark current of 10 e/s and a readnoise of 5 e RMS), the sensitivity is 50σ1s = 14.8 Z, which meets easily the requirement. A neutral density filter is required to guide on the brightest RV targets (calibrations stars). CCD integrations of up to a minute satisfy all the acquisition and guiding requirements of the secondary science cases. For example, see the GRB observing scenario in the OCDD.

5. INSTRUMENT DESCRIPTION

5.1 OVERVIEW

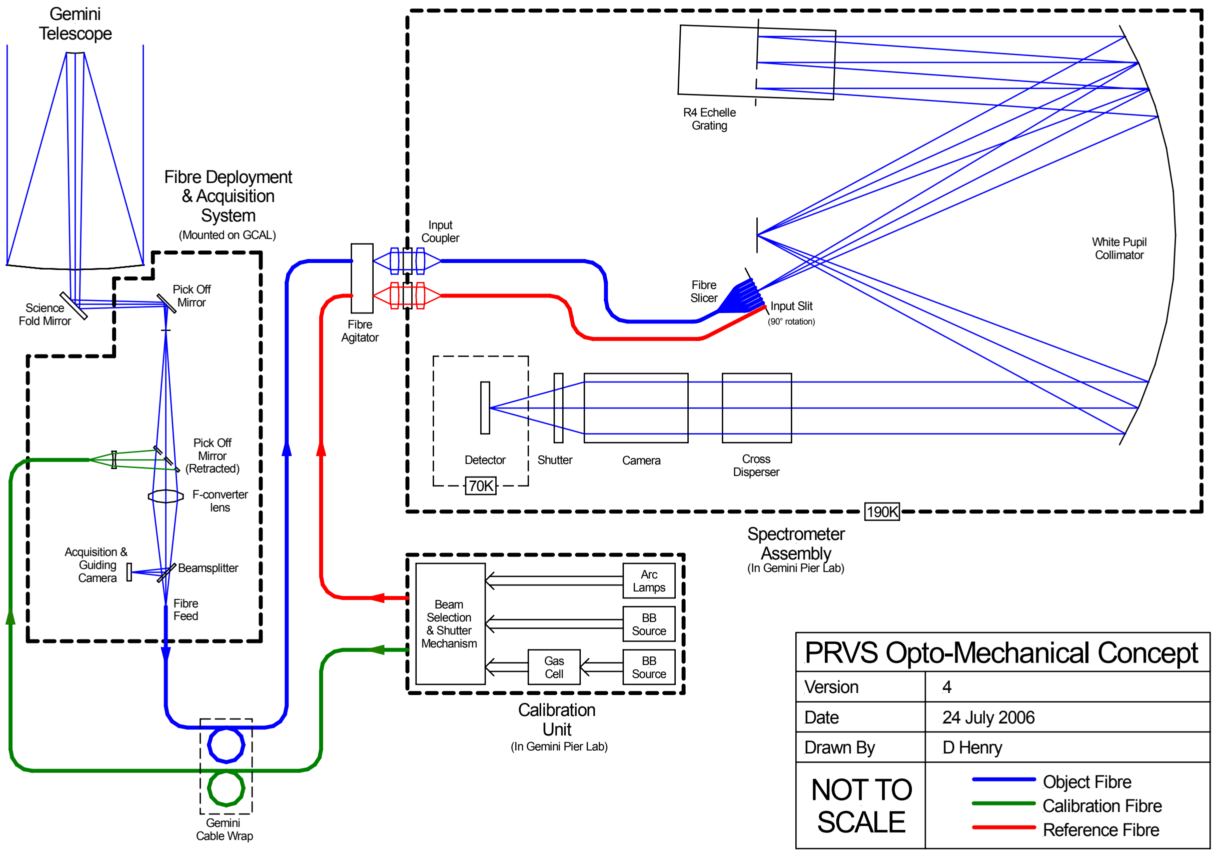

Figure 6. Schematic layout of PRVS

Light from the telescope is re-imaged onto the entrance of an optical fibre located in the Fibre Deployment and Acquisition System (FDAS) which is mounted on the ISS near to the GCAL unit at the f/16 cassegrain focus. A CCD fibre-viewing camera is used for acquisition and guiding. The 60 m long ‘object’ fibre runs from the FDAS through the telescope cable wrap down to the telescope pier laboratory and into a bench-mounted spectrograph. For environmental stability the spectrograph is contained inside a vacuum jacket and is temperature controlled. The bulk of the spectrograph is cooled to 190 K. A second ‘reference’ fibre runs from a calibration unit located next to the cryostat into the spectrograph. A third ‘calibration’ fibre feeds calibration light up to the FDAS so that calibration light can also be transmitted through the object fibre when selected. The object and reference fibres are terminated at the cryostat and optically coupled into the cryostat to form a pseudo-slit at the entrance of the spectrograph. Starlight from the object fibre is dispersed in the spectrograph and forms the object spectrum side-by-side with a wavelength reference spectrum formed by dispersed arc line light from the reference fibre.

Radial velocity is measured by measuring the wavelength shift of the object spectrum relative to the simultaneously exposed wavelength reference spectrum. Figure 6 shows a schematic layout of PRVS.

5.2 FIBER DEPLOYMENT AND ACQUISITION SYSTEM

The Fibre Deployment and Acquisition System is mounted on the ISS close to GCAL. This system re-images the telescope focal plane onto the object fibre and uses a CCD camera (the Fibre Viewer) for object acquisition and slow guiding. It also projects calibration light into the object fibre when required.

The science fold mirror sends the beam to the FDAS where a small pickoff mirror sends the f/16 beam to a focal reducing achromatic doublet lens (see Figure 6). This lens re-images the telescope focal plane at f/5.5 onto the object fiber. A focal ratio of f/5.5 is chosen to minimize focal ratio degradation. The fibre is 300 μm in diameter and only uses 1.4″ of the re-imaged field. For median seeing of about 0.6″ at J the light loss (spill-over from the object fibre) is about 2%.

A CaF2 substrate located behind the lens reflects about 1.5% of this beam through a Z-band (0.83-1.00μm) filter and onto a CCD (the Fibre Viewer). The bare substrate reflects enough signal for acquisition and guiding on our faintest RV targets (L2 dwarf at ~6 pc, 50σ1sec=14.8 at Z, 50% QE) while at the same time minimizing the light loss in the spectrograph path. The brightest stars in the RV survey are early M dwarfs (Z magnitude <5.0) and require additional filtering (Z plus neutral density filter) to avoid saturation in the shortest on-chip integration times of about 0.1 s. This requires a simple filter wheel or slide in front of the CCD camera.

There is a small position offset between the guiding (Z) and observing wavelengths (YJH) due to atmospheric dispersion (about 0.15″ between Z and J at an airmass of 1.5). This is corrected for in software. At an image scale 0.06″/pixel (13μm) a 512x512 CCD format gives a FOV 31″x31″. The lens, substrate, fibre, and CCD are all rigidly mounted and so there is no significant relative flexure (< one CCD pixel/hour). Any flexure in the pickoff mirror acts like a simple guiding error.

When the pickoff mirror is in its retracted position the output of the calibration fibre is re-imaged onto the input of the object fiber at f/5.5. Calibration light (arcs, continuum, continuum plus gas cell absorption) in the object fibre is observed before and after observing the science object.

Several off-the-shelf CCD camera (CCD, dewar, thermoelectric cooler, driver) systems are currently being considered. If space is constrained around GCAL we could build our own system.

Fast guiding for windshake is provided by the PWFS and slow guiding for flexure compensation between the PWFS and object fibre is done with the FV CCD. The slow corrections from the FV go via socket communication to the telescope control system. The PWFS also corrects for astigmatism and slow focus changes.

The acquisition and guiding procedure is as follows:

1. Short slew of telescope to target, pointing ± 2″
   (≈1 min)

2. Image with FV and offset to centre of fibre (calibrated in CCD pixel co-ordinates), pointing ±0.1″.
   (≈1 min)

3. Acquire offset star with PWFS. Start fast guiding PWFS (100Hz sampling, ≈30Hz correction).
   (≈2 min for WFS loop to converge.)

4. Start slow guiding with FV (1Hz sampling, ≈0.3Hz correction). Slow guiding can start before the WFS loop has converged.

5. Start spectrograph integration. Typical integration times range from a few minutes to one hour

Since object integration times are typically about 15 minutes (14 min for S/N=300 on m_Y=10.5 M6 V *v*sin*i*=5 km/) the object acquisition time needs to be not longer than a few minutes to maintain an observing efficiency of better than 80% over the course of the RV survey (100 nights per year for five years is proposed, see OCDD).

For details see the Fibre Deployment and Acquisition System Document (ref - PRVS-TRE-00007-0001).

5.3 FORE-OPTICS FIBRE ASSEMBLY

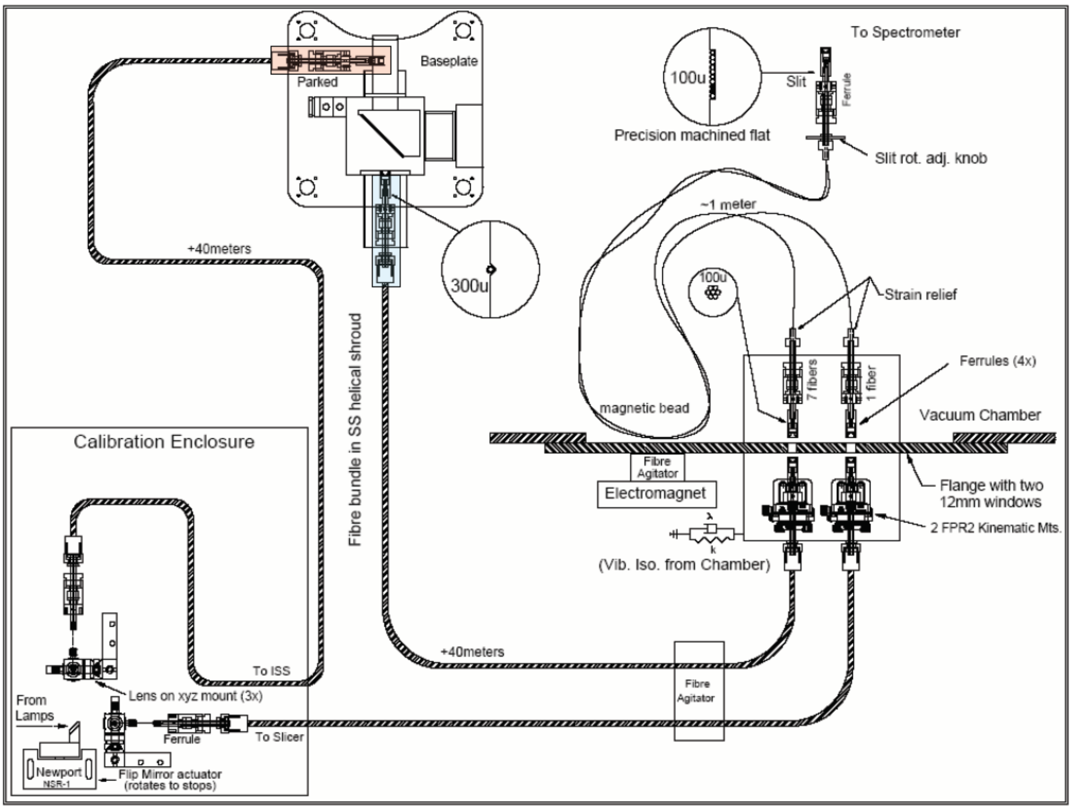

Figure 7 Layout of the Fore-Optics Fibre Assembly

Starlight from the telescope focal plane is re-imaged onto the end of the object fibre at a focal ratio of f/5.5 to minimize focal ratio degradation. The 300 μm diameter object fibre runs from the FDAS through the cable wrap to the cryostat located in the telescope pier laboratory, requiring a fibre length of about 60 m. The 100 μm diameter reference fibre runs from the Calibration Assembly to the cryostat, requiring a length of a few meters. The calibration fibre runs from the Calibration Assembly to the Fibre Deployment and Acquisition Assembly next to GCAL, along the same path as the object fibre. See Figure 7.

The object and reference fibres are terminated at the cryostat and optically coupled into the cryostat by individual collimator and camera lenslets. The reference fibre is re-imaged onto a 100 μm diameter fibre, and the 300 μm diameter object fibre is re-imaged onto a bundle of seven 100 μm diameter fibres that is then is splayed out to form a long pseudo slit at the entrance of the spectrograph (see Figure 8). The reference fibre is added to the top of the pseudo slit. To minimize any scattering of arc light onto the object spectrum at the detector one blank fibre of the same diameter separates the reference and object fibres.

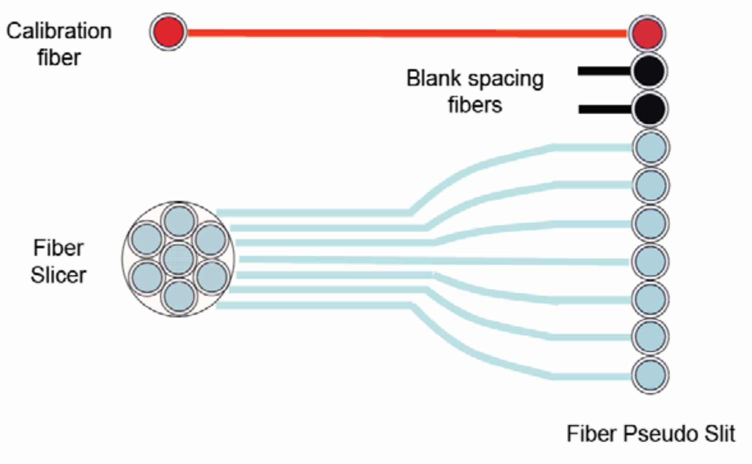

Figure 8 Fibre image slicer and pseudo slit

Immediately outside the entrance to the cryostat the object and reference fibres pass through a mechanical agitator to remove modal noise and to increase spatial scrambling. This device agitates the fibres at a frequency of about 60 Hz and at an amplitude of a few hundred microns. There is about 1 m length of fibre from the image slicer input to the pseudo slit. To remove modal noise this cable is run through magnetic beads that are slightly vibrated through the cryostat vacuum jacket via an electromagnet outside the jacket.

For details see Fore-Optics Fibre Assembly Document (ref - PRVS-TRE-00002-0001).

5.4 SPECTROGRAPH

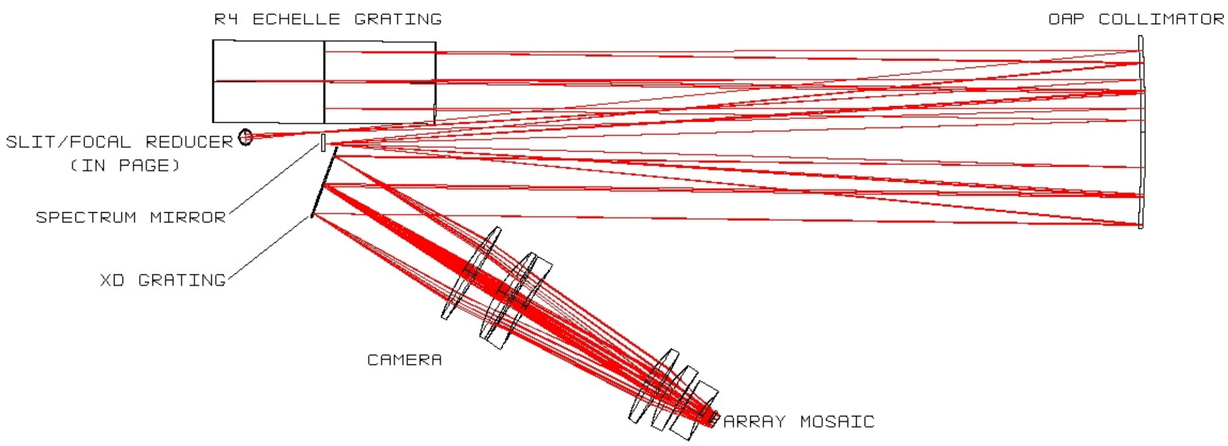

Figure 9. Spectrograph layout

The optical design of the spectrograph is similar to other white pupil spectrographs such as UVES on the VLT, MRS on the HET and, in particular, HARPS on the ESO 3.6m La Silla telescope. The layout of the spectrograph is shown on Figure 9. The f/5.5 beam exiting from the pseudo-slit is reduced to about f/14 by the focal reducer doublet lens. The slower beam is needed to control aberrations in the spectrograph. A large off-axis parabolic (OAP) mirror then collimates the beam and forms a 140 mm diameter white pupil on the echelle grating. The OAP collimator has a focal length of 2000 mm and a rectangular clear aperture of 500 mm x 446 mm. For thermal stability all the mirrors and gratings are made from Zerodur.

For a resolving power of R=70,000 an R4 31.6 lines/mm echelle grating is required (162 mm x 552 mm). This is the same as used in HARPS, UVES and some other spectrographs. Grating illumination is in pseudo-Littrow mode with an off-plane angle of γ =0.4°. This is optimum for throughput but does introduce a small tilt of about 3° of the re-imaged slit on the detector.

Following dispersion at the grating a second reflection in the OAP forms a dispersed image of the slit on the spectrum mirror (clear aperture 386 mm x 30 mm) that is located next to the echelle. The beam from the spectrum mirror is reflected for a third time in the OAP and forms a second white pupil on the cross-dispersing grating located close to the spectrum mirror. The cross-disperser is a first-order plane grating (100 lines/mm, blaze angle 4°). It is tilted 20° to allow the reflected beam to clear the input beam.

The dispersed beam from the cross disperser is imaged onto the array mosaic by a six-element f/3 refractive camera. All the lenses have spherical surfaces and are made from standard optical glasses with diameters ranging from about 100 mm to 260 mm. An order-sorting filter is the last optical element before the detector. Image quality at the detector is very good with RMS spot diameters < 9 μm (including tolerancing) compared to the re-imaged slit width at the detector of 45 μm (2.5 pixels). Therefore the spectrograph image quality only degrades the resolving power by 2%.

In the baseline design a 1x2 mosaic of H2RG 2048x2048 detectors (18μm pixels) covers most of the YJH spectral range simultaneously at R=70,000 with 2.5 pixel sampling, and with sufficient separation between orders to accommodate the image-sliced slit containing the object and reference fibres.

For details see the Spectrograph Assembly Document (ref - PRVS-TRE-00003-0001).

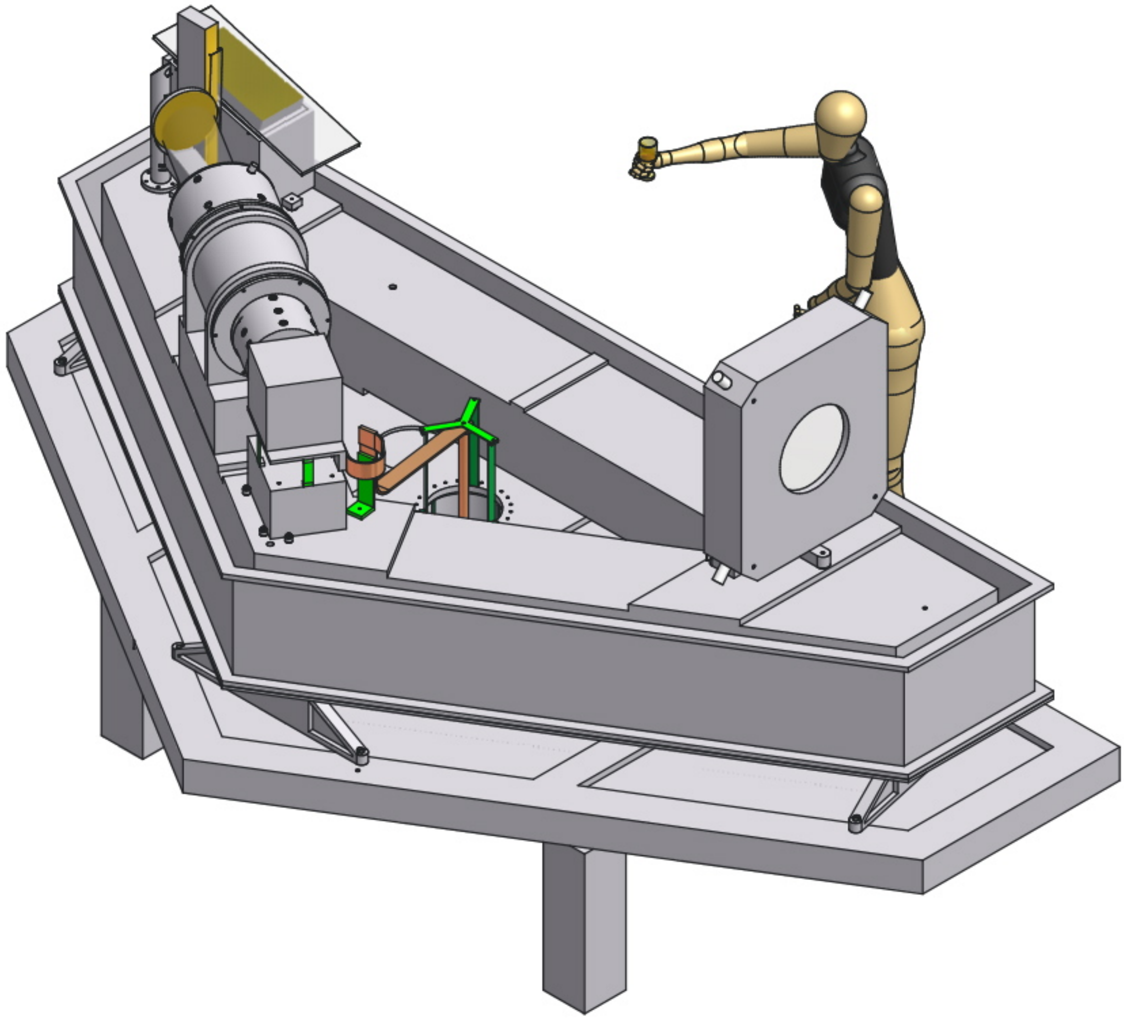

Figure 10. Cryostat optical bench and support structure

5.5 CRYOSTAT

The design consists of a vacuum vessel (~3.3 m x 1.7 m x 1.25 m, volume 2.8 m^3) supported on anti-vibration supports of the type used on optical benches (see Figures 10 and 11). An optical support structure is mounted within the vacuum vessel on an isolating flexure system. The flexure system supports a radiation shield that encloses the optical support structure. It also thermally insulates the optical support structure from the radiation shield. The optical components are mounted within substructure modules, and these in turn are mounted to the optical support structure in a semi-kinematic way. The optical bench and radiation shield are maintained at the operating temperature of 190 K and stabilised to better than 0.05 K by combining a vibration-isolated CTI-1050 closed-cycle cooler with servo controlled resistive heating elements on the optical bench. Liquid Nitrogen plumbing and a dewar is provided to pre-cool the radiation shield and the optical bench. The second stage of the closed-cycle cooler maintains the array mosaic at ~70 K and stabilised to around 0.01 K. A window/feed-through provides the interface for the fibre coupling. There are also breakout panels for the instrument vacuum services, electrical services and detector signal cabling.

The total mass of the cryostat is 1705 Kg, comprising of the cold structure 863 Kg (optical bench and components 411 Kg, radiation shield 452 Kg), vacuum vessel 747 Kg, legs 45 Kg, and fasteners 50 Kg.

For details see the Infrastructure Document (ref - PRVS-TRE-00001-0001).

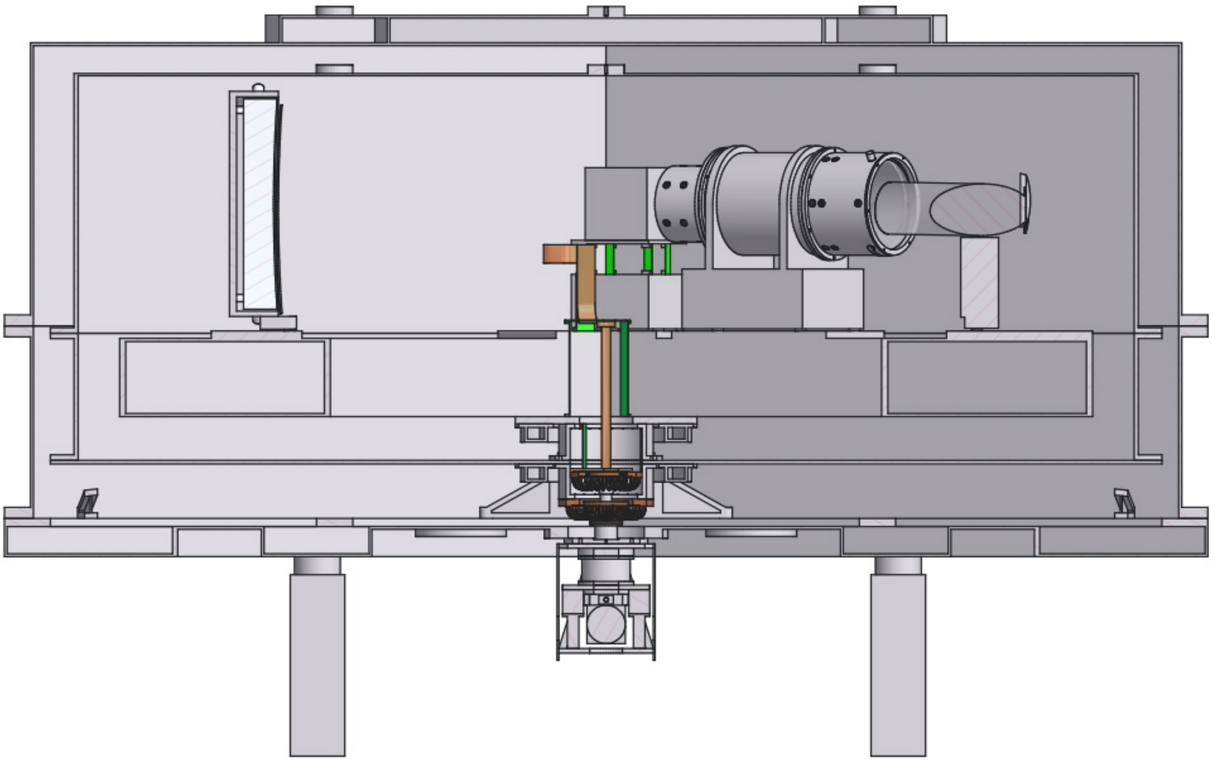

Figure 11. Cryostat cross-section showing the optical bench, radiation shield, vacuum vessel, closed-cycle cooler, and support structure

5.6 CALIBRATION ASSEMBLY

The Calibration Assembly (see Figure 12) is located next to the cryostat in the pier laboratory. It contains a set of five arc lamps (Krypton Neon, Xenon, and two Thorium-Argon lamps) for standard wavelength calibration, a continuum lamp for flat fielding, and a continuum source with gas cell absorption for additional calibration. The output of the lamps is coupled into fibres and routed either to the calibration fibre or the reference fibre. The arc lamps are optically combined together to provide about 300 bright lines for simultaneous wavelength calibration (to track wavelength shifts) while observing the RV targets. These same arc lamps provide thousands of lines for SRF measurement and wavelength solution during daytime calibration. During daytime calibration a series of different integration times can be used for measurements of both bright and faint arc lines. The second Th-Ar lamp is not used during observing but only during daytime calibration to extend its lifetime. It provides a ‘gold standard’ wavelength reference when the other lamps need to be replaced. The gas cell provides another (limited range) absolute wavelength reference to track any changes in calibration when the arc lamps are replaced. The calibration assembly enclosure is temperature controlled for wavelength stability. The use of the calibration assembly during observing and calibration is described in the OCDD.

For details see the Calibration Assembly Document (ref - PRVS-TRE-00004-0001).

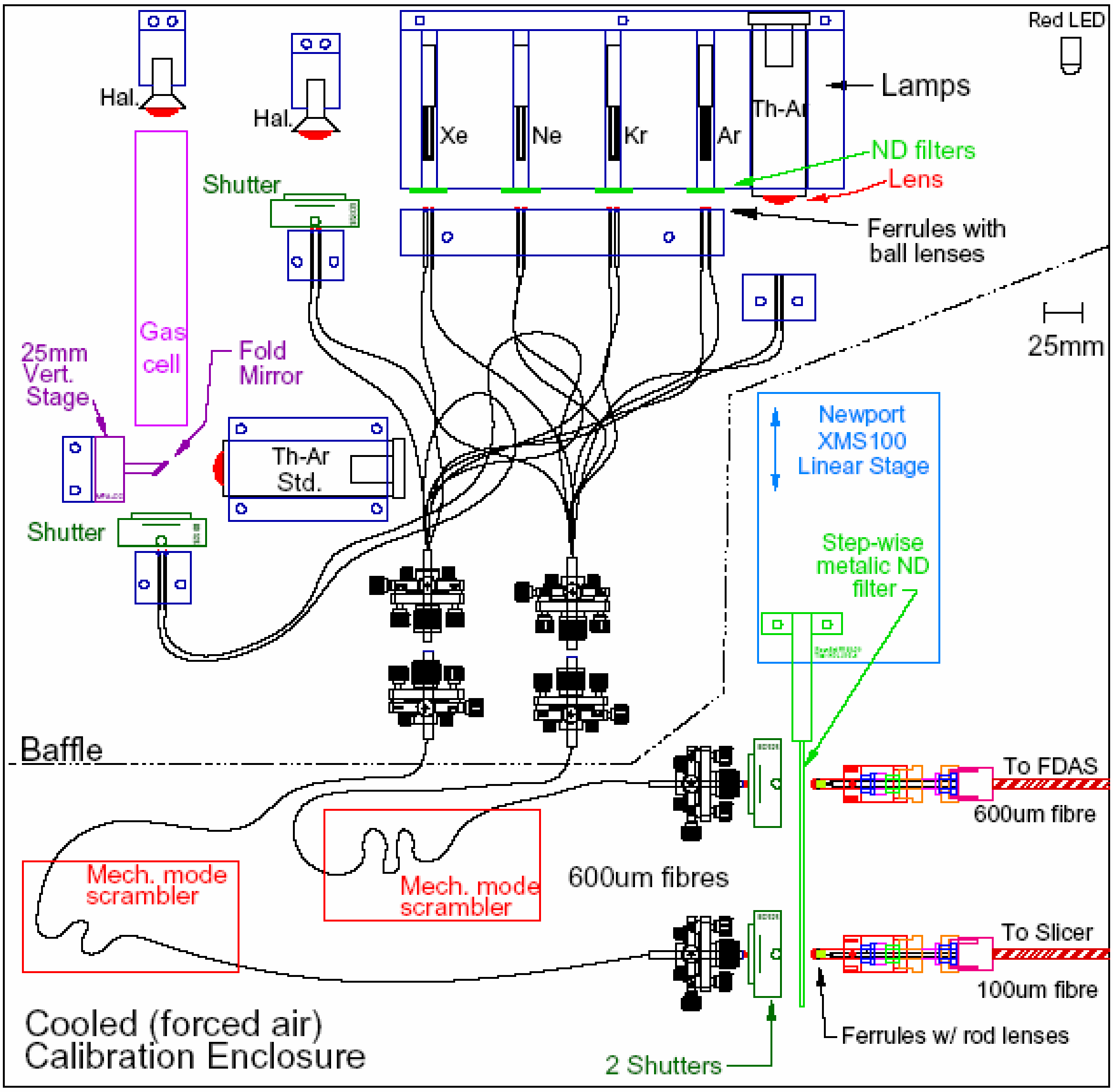

Figure 12. Layout of the Calibration Assembly and the fibre connections to the fibre deployment system at cassegrain focus and the cryostat

5.7 INSTRUMENT CONTROL

The instrument control sub-system performs top-level configuration and control of other sub-systems. It provides user interfaces and consists of software components that plug in to Gemini software. The sub-system is primarily software but will run on two workstations (see Figure 13). One will be located in the telescope dome and will convert the output from the acquisition camera into an offset for the telescope and will control the mechanism that drives the pick-off mirror into the field. The other will be located in the Pier lab and will contain the rest of the instrument control functions. The control software for PRVS is based around Internet appliances; a central instrument sequencer will use existing Applications Programmer Interface's to talk to Galil motion controllers, Lakeshore temperature controllers and Ultracam camera readout systems. We have successfully used these components in previous instruments. The central system uses the Gemini Instrument Applications Programmer Interface for all command and control from higher-level systems, and a remote storage system for data handling.

A list of the mechanisms controlled is given in Table 8. The mechanisms are all independent and so can be reconfigured at the same time.

Fibre Deployment and Acquisition System
Deployable pick-off mirror
Filter exchanger
Fore-optics Fibre Assembly
External fibre agitator
Internal fibre agitator
Calibration Assembly
Flat-field Halogen lamp shutter
Gas cell Halogen lamp shutter
Kr arc lamp shutter
Ne arc lamp shutter
Xe arc lamp shutter
Ar arc lamp shutter
#1 Th-Ar lamp shutter
#2 Th-Ar lamp shutter
Flip mirror in/out
Spectrograph
Detector shutter

Table 8 List of Mechanisms

For details see the Instrument Control System Document (ref - PRVS-TRE-00006-0001).

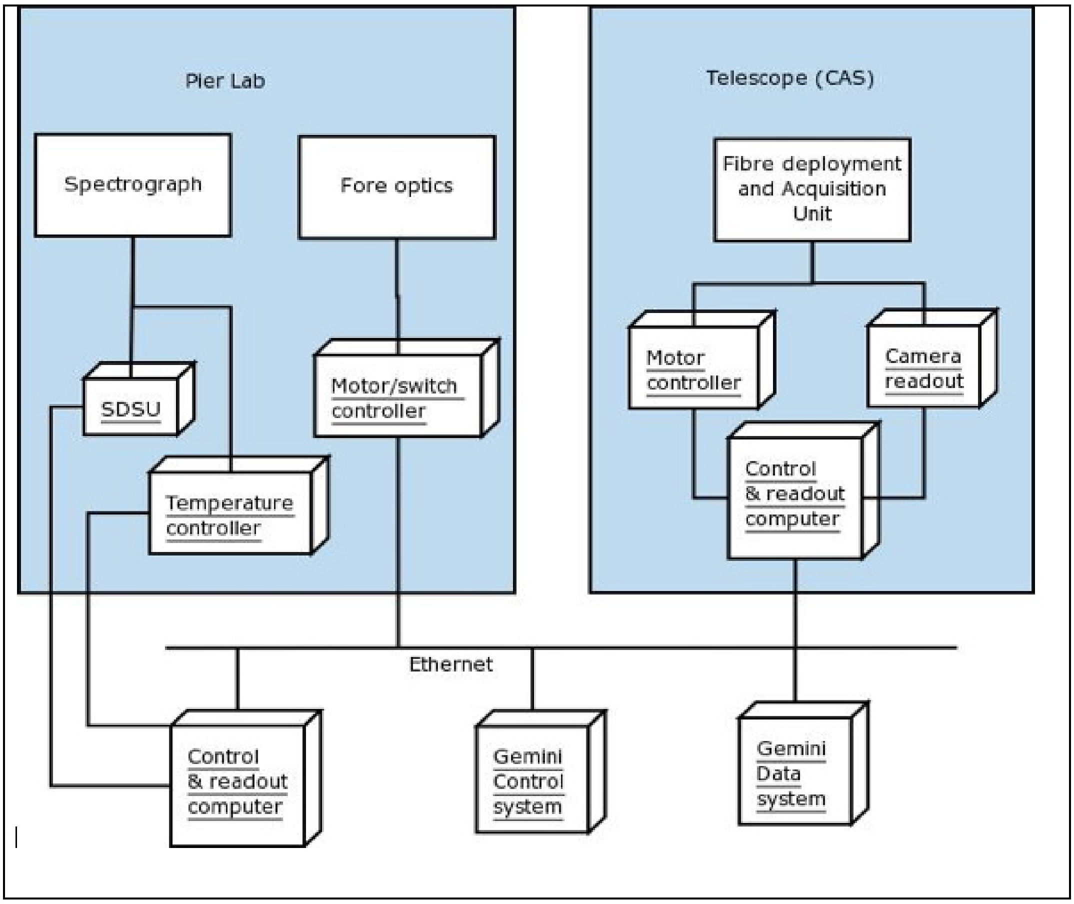

Figure 13. Instrument Control Architecture

5.8 DATA REDUCTION PIPELINE

The Data Reduction pipeline for PRVS will need to reduce multi-order spectral data with emphasis on line extraction and centroiding. In order to maximize the effectiveness of the instrument considerable care must be taken in the preparation and use of calibrations. Optimal extraction routines combined with careful artifact removal will be used to provide data suitable for direct use by radial velocity estimation codes. In addition, quality control checks of short and long-term instrument stability will be provided, along with recipes to pre-process calibration data.

For details see the Data Pipeline Document (ref - PRVS-TRE-00005-0001).

6. COMPLIANCE SUMMARY

The design analysis performed so far indicates the following expected performance against the primary Science requirements (Table 9).

Requirement		Essential	Predicted
SR_1	Radial Velocity	3 m/s	2 m/s (see Table 9)
SR_2	Sensitivity	Y>11.75, J> 11.25, H>10.75 for S/N = 300 in 3600 s	Y=12.00, J=11.44, H=10.91 S/N =300 in 3600 s
SR_3	Observational Efficiency	> 70% in 3600 s	80% in 3600 s
SR_4	Spectral Resolving Power	> 50,000	70,000
SR_5	Sampling	2.5 pixel	2.5 pixel
SR_6	Simultaneous wavelength Coverage	$\geq$ 80% of Y+J+H bands (not including telluric mask)	90% of Y+J+H bands (not including telluric mask)
SR_7	Instrument SRF stability	0.1 pixel drift (5 K change) skewness $\pm$ 0.001 ($\pm$0.05K)	< 0.01pixel ($\pm$0.05K) $\pm$ 0.001 ($\pm$0.05K)
SR_8	Throughput	5%	10%
SR_9	Field of View	> 1.2″	1.4″
SR_10	Instrument Background	< 0.2 e/s	< 0.1 e/s if no persistence
SR_11	Acquisition and guiding	< 0.1″	< 0.1″
SR_12	Guiding sensitivity	Z>14.8 for S/N=20 in 1 s	Z>14.8 for S/N=50 in 1 s
SR_13	Image quality at fibre	50%EED <2 pixel	50%EED = 1 pixel
SR_14	Image quality at detector	50%EED <0.8 pixel	50%EED=0.5 pixel
SR_15	Array Cosmetic Quality	<3%	<1%

Table 9 Compliance Summary

7. RADIAL VELOCITY ERROR BUDGET

A preliminary estimate of the radial velocity error budget is given in Table 10. From the modelling of the arc lines in the Science Case the measurable precision per line at about full well (50,000 e) is 6 m/s. About 300 arc lines provided by Th-Ar, Ne, Kr, and Xe lamps can be measured in 10 s, improving the precision for measuring any wavelength drift between the object spectrum and reference spectrum to 0.35 m/s. Typical integration times on the science object are longer than one minute, improving the precision to better than 0.14 m/s. To relate these wavelength drift measurements to other object spectra requires wavelength calibration. Wavelength calibration is done during the daytime calibration procedure. During daytime calibration more time (~ one hour) is available to take a series of exposures on Th-Ar, Kr, Ne, and Xe lamps, varying the integration time so that more than 1000 lines can be measured resulting in precisions better than about 0.1 m/s.

The same measurements required for wavelength calibration are also used to measure the instrument SRF. The skewness of the instrument SRF needs to be measured to better than 0.001 for this component of the RV noise to be better than 0.3 m/s; see the detailed discussion of the modelling in the Science Case. Any opto-mechanical drift of the spectrum on the detector needs to be less than 0.1 pixels, due to changes in skewness that would result, in a precision of better than 0.3 m/s.

Centring errors of the science object on the input fibre also affect RV precision. The spatial scrambling properties of the fibre (>1000 from mechanical agitation and dual fibre optical scrambling) and guiding with the Fibre Viewer (1.4″to 0.1″) reduce these errors by a factor of more than 14,000, i.e. from 4,300 m/s (R=70,000) to less than 0.31 m/s. Changes in the background can affect the RV by changing the S/N detection on the source. If the estimated background of 0.1 e/s increases by a factor of two then the detected S/N changes from a nominal S/N=300 (~M9 V in 3600 s) to S/N=280, equivalent a RV error of about 0.1 m/s. This is considered an upper limit since most stars are brighter, the background will probably be lower, and the change in background is pessimistically high.

Atmospheric noise is estimated by offsetting telluric features selected from a Gaussian distribution of ± 100 m/s due to variations high altitude winds in model M dwarf spectra. Telluric features deeper than 2% are then masked out and the radial velocity of ten otherwise identical spectra measured. The dispersion of 0.5 m/s is an estimate of the telluric jitter during an observation.

The source photon noise comes from the modelling in the Science Case. The 1 σ velocity precision is therefore $(1.50^2 + 0.75^2)^{0.5}$ m/s = 1.68 m/s for a typical RV survey target star (M6 V), not including any intrinsic noise.

Error source	**Contribution**	**Comment**
Drift measurement with sim. arcs	< 0.14 m/s	~ 300 arc lines typically > 60 s
Wavelength calibration	< 0.1 m/s	> 1000 arc lines during daytime calibration
Instrument SRF measurement	< 0.3 m/s	> 1000 arc lines during daytime calibration
Opto-mechanical stability	< 0.3 m/s	< 0.1 pixel drift during an observation
Centring and guiding	< 0.3 m/s	Spatial scrambling of fibre and CCD guiding
Background subtraction	< 0.1 m/s	Stability of background, dark current, bias etc.
Atmospheric noise	~ 0.5 m/s	Modelled effects of telluric jitter
Total non-source noise	**< 0.75 m/s**	RMS

Source photon noise	**1.5 m/s**	m_Y=10.5 M6 V (*v*sin*i*=5 km/s) at 10 pc S/N=300 in 14 min
Source radial velocity jitter	(0-100 m/s)	Sources will be selected for minimum radial velocity jitter
Total noise (1 σ)	**1.7 m/s**	For typical M6 V star at 10 pc (no radial velocity jitter)

Table 10 Error budget for PRVS radial velocity measurements

8. RE-USE

The philosophy of the design has been to assiduously avoid R&D where possible and to re-use designs that are known to work in order to minimise risk and hence cost. Table 11 indicates the areas of the design that have been taken over or adapted from other instruments that our institutions have been involved with or are available commercially.

Assembly/component	**Used In**	**Comments**
Fibre Viewer camera	Commercial off-the-shelf	
Detector shutter	SCUBA2	
R4 echelle	Commercial off-the-shelf	
H2RG detector, mosaic mount	WFCAM, NSFCAM2, ULBcam	Windowed readout demonstrated
Detector Controller	WFCAM	SDSU controllers used routinely in infrared instruments at UK ATC
Strong temperature control of cryostat and detector	ULBCam, NIRI	Lakeshore controllers used routinely in infrared instruments
Cryostat	WFCAM, SCUBA 2	Standard UK ATC approach
Instrument control	GMOS, NIRI	Standard techniques for Gemini instruments developed at UK ATC and UH
Fibre feed	HET spectrographs	Standard Penn State approach

Table 11 Re-use of components and designs in PRVS